JOURNAL OF VIROLOGY, June 1995, p. 3878–3884 Vol. 69, No. 6
0022-538X/95/$04.00+0

Domains Upstream of the Protease (PR) in Human Immunodeficiency Virus Type 1 Gag-Pol Influence PR Autoprocessing

GABRIELE ZYBARTH AND CAROL CARTER*

Department of Microbiology, State University of New York at Stony Brook, Stony Brook, New York 11794

Received 6 April 1994/Accepted 17 March 1995

A critical step in the formation of infectious retroviral particles is the activation of the virally encoded protease (PR) and its release from the Gag-Pol precursor polyprotein. To identify factors that influence this step, the maturation of human immunodeficiency virus type 1 PR from various Gag-PR polyproteins was assayed in vitro by a using rabbit reticulocyte lysate as a coupled transcription-translation-autoprocessing system. Highly efficient autoprocessing was detected with polyproteins containing the viral nucleocapsid (NC) domain. In contrast, polyproteins consisting of only p6* and PR domains or containing a truncated NC domain exhibited no autoprocessing activity. Experiments designed to test the dimerization capability of short PR polyproteins revealed that precursors containing the NC domain exhibited very efficient homotypic protein-protein interactions while PR precursors consisting of only p6* and PR did not interact efficiently. The strong correlation between autoprocessing activity and PR polyprotein precursor dimerization suggests that NC and p6* domains play a role in PR activation by influencing the dimerization of the PR domain in the precursor.

All retroviruses express their structural and enzymatic functions as precursor polyproteins, designated Gag and Gag-Pol, respectively (33). In human immunodeficiency virus type 1 (HIV-1), the Gag precursor contains domains for the matrix (MA), capsid (CA), p2, and nucleocapsid (NC) as well as two C-terminal domains, p1 and p6 (35). Gag-Pol precursors are generated after a rare ribosomal frameshift event which occurs at the NC-p1 junction (11). Gag-Pol precursors therefore consist of MA, CA, and NC domains followed by the transframe domain (p6*), protease (PR), reverse transcriptase, and integrase. Both types of precursors are assembled into viral particles and processed by the virus-encoded PR. An important step in the life cycle of retroviruses is the activation of PR since inhibition of polyprotein precursor processing results in immature and noninfectious virus particles (13, 15). In the case of HIV, the important role of PR in the formation of infectious virions has made it the focus of intense investigations. Active HIV-1 PR is a dimer of two identical 11-kDa monomers, each providing one of the two Asp-Thr-Gly (DTG) sequences at the active center of aspartic PRs (36). The cellular and fungal members of the family of aspartic PRs are monomeric proteins with two DTG-containing domains. Their activation is mostly regulated by N-terminal pro-sequences (e.g., pepsinogen [12]). The mechanism of activation of retroviral enzymes has not been elucidated. In type C viruses and lentiviruses, which assemble at the plasma membrane, premature PR activation is believed to be prevented by the limited concentration of Gag-Pol precursors in the cytoplasm. Since each Gag-Pol precursor contains only one PR domain, Gag-Pol precursor dimerization is necessary for the formation of the PR active site. However, additional mechanisms of regulation must be present during assembly and budding because HIV Gag-Pol precursors can undergo autoprocessing in the cytoplasm of some cells and in some in vitro systems (14, 16, 28). Moreover, in type C viruses, PR activation does not occur before the viral particle is completely released from the host cell even though viral precursors are highly concentrated at this stage (33). In addition, type B and type D retroviruses assemble their particles entirely intracytoplasmically but do not activate the PR function until the particles are released from the host cell (27).

In the avian type C retrovirus Rous sarcoma virus, a region in Gag was speculated to function as a negative regulator of PR activation (2). In HIV-1, the transframe region (p6* domain) may be involved in PR activation since deletion of this domain increases the autoprocessing activity of Gag-PR precursors in vitro (25). In this study we report a further characterization of the effect of regions immediately upstream of PR on autoprocessing and precursor dimerization.

Autoprocessing of Gag-PR precursors. To analyze autoprocessing, constructs were designed to express polyproteins containing the wild-type PR domain preceded by upstream sequences of increasing lengths (Fig. 1). Control constructs encoded a PR domain containing an inactivating mutation of the catalytic Asp-25 residue to Ala (PRA). All inserts were cloned into the unique *Bam*HI site of vector pET3 under the control of the promoter for T7 RNA polymerase (30). Insertion at *Bam*HI results in in-frame fusion with sequences coding for the first 11 amino acids from bacteriophage T7 gene 10 plus an arginine specified by the linker sequence for *Bam*HI. This T7 tag provides the methionine start codon for all constructs. To study only the effects of upstream sequences on PR activity, a stop codon was placed at the C terminus of the PR-coding region. The exclusive synthesis of PR-containing precursors was ensured by introducing 4 bp next to the natural frameshift site (16). Plasmids were grown in *Escherichia coli* C600 and JM101, and DNA was prepared by using the Promega Magic Mini Prep system. To ensure uniform translational efficiency of all constructs, equal amounts of supercoiled DNA were then used to direct transcription and translation in TNT T7 rabbit reticulocyte lysate (RRL; Promega) in the presence of [^{35}S]methionine (specific activity, >1,000 Ci/mmol; ICN). Incubation

* Corresponding author. Mailing address: Department of Microbiology, SUNY at Stony Brook, Stony Brook, NY 11794-8621. Phone: (516) 632-8801. Fax: (516) 632-8891. Electronic mail address: carol@asterix.bio.sunysb.edu.

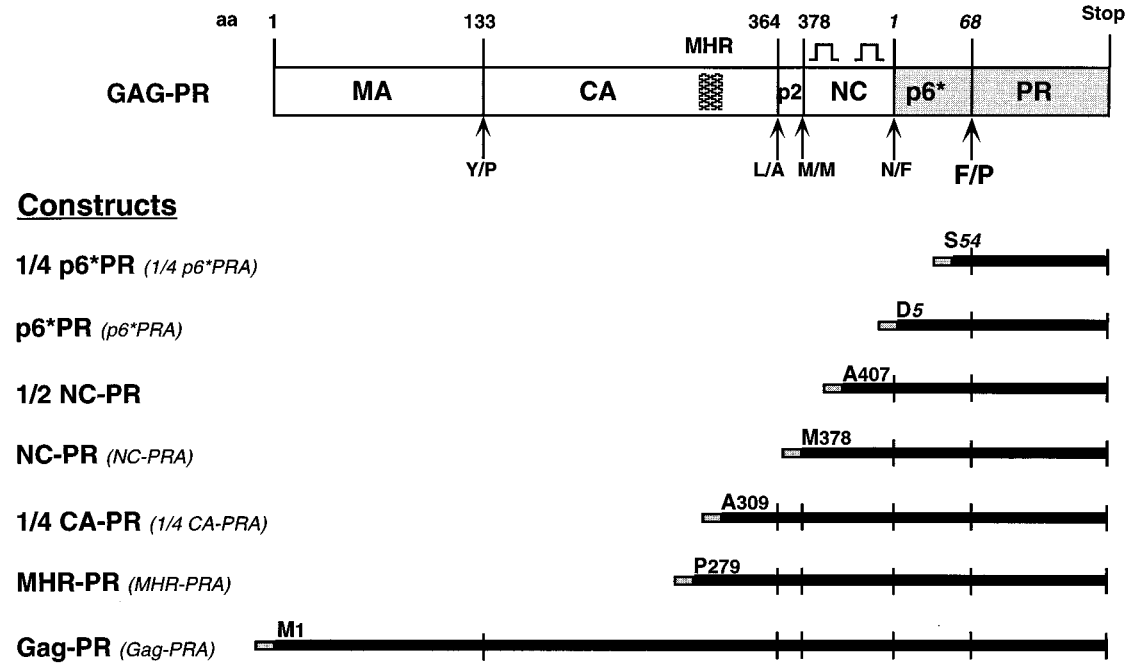

FIG. 1. Extended precursors used for analysis of autoprocessing. A schematic representation of the parental Gag-PR polyprotein precursor is shown at the top. Open boxes represent Gag domains (MA, CA, p2, and NC); shaded boxes represent Pol domains (p6* and PR). The number of the amino acid (aa) at the start of each domain is given (HIV-1 strain BH10 [26]). Amino acid numbers in the Pol domain are in italics. PR cleavage sites between domains (arrows) are identified by the residues flanking the scissile bond. The hatched region in CA and the symbols above NC denote the major homology region (MHR) (35) and the Cys-His motifs, respectively. The bars below show the domains present in the extended constructs. The first amino acid encoded at the beginning of each precursor and the PR cleavage sites present in the precursors are indicated. The small shaded boxes represent the T7 tag sequence (30). Control constructs, denoted as *PRA*, contain an inactivating mutation of the PR active site residue Asp-25 to Ala. p6*PR and p6*PRA, plasmids gpII and gpIIA (16), respectively, were cut with *Bgl*II and *Eco*RI. The resulting 494-bp fragments were ligated into the pET3c vector which had been digested with *Bam*HI and *Eco*RI. 1/2 NC-PR, a linker containing a *Bam*HI restriction site was inserted at the *Apa*I site (nucleotide 1555 of BH10) of plasmid FSIII (24). The resulting construct was digested with *Bam*HI and *Eco*RI, and the 583-bp restriction fragment was subcloned into pET3b. 1/4 p6*PR, 1/4 p6*PRA, NC-PR, and NC-PRA, inserts were generated by PCR from template plasmid FSIII and FSIIIA, respectively. Synthesis at the 5′ ends of the inserts for 1/4p6*PR and 1/4p6*PRA was primed by oligonucleotide CGGGATCCTCAGAAGCAGGAGCCG, which annealed at nucleotides 1786 to 1803 (BH10). The 5′ primer for NC-PR and NC-PRA, CGCGGATCCATGCAGAGAGGCAATTTTAGG, annealed at positions 1465 to 1485 (BH10). Both primers also contained a *Bam*HI site. Synthesis at the 3′ ends of all four inserts was primed with the M13 reverse primer (Stratagene). The resulting PCR fragments were digested with *Eco*RI and *Bam*HI and inserted into pET3a. 1/4 CA-PR, 1/4 CA-PRA, MHR-PR, and MHR-PRA, PCR fragments primed at the 5′ ends with oligonucleotide CGCGGATCCGCTTCACAGGAGGTAAAAAATTGG, nucleotides 1258 to 1281 (1/4 CA-PR and 1/4 CA-PRA), and with oligonucleotide CGCGGATCCCCTACCAGCATTCTGGAC, nucleotides 1168 to 1185 (MHR-PR and MHR-PRA), were synthesized. The oligonucleotide for the 3′ end was complementary to the *Apa*I site (nucleotide 1555). Both fragments were digested with *Bam*HI and *Apa*I and exchanged with the *Bam*HI-*Apa*I insert of NC-PR and NC-PRA. PCRs were carried out in a thermal cycler (Perkin-Elmer) with Vent DNA polymerase (New England Biolabs) under conditions recommended by the supplier. All PCR-derived sequences were confirmed by sequencing.

conditions were as recommended by the supplier, at 30°C for 1 h. This in vitro system was selected over other expression systems because it represents an efficient and sensitive assay for HIV-1 PR autoprocessing activity in an eukaryotic background (3). It permits the analysis of processing products and transient intermediates which might be unstable or undetectable in tissue culture or in *E. coli* expression systems.

Translation products were analyzed either directly by sodium dodecyl sulfate-polyacrylamide gel electrophoresis (SDS-PAGE) or after immunoprecipitation (17, 24). Translation reactions directed by the control construct Gag-PRA, which contains an inactivating mutation of the catalytic aspartic acid residue of PR (D-25 to A), accumulated full-length precursor Pr69 as the primary translation product along with several smaller proteins that are most likely the products of internal initiation or premature termination (Fig. 2A, lane 1). Since Gag-PRA exhibits no proteolytic autoprocessing, immunoprecipitation with an antibody directed against PR detected only full-length and internally initiated products (Fig. 2A, lane 2). Products presumed to be prematurely terminated were identified by immunoprecipitation with antibodies directed against the T7 tag sequence, CA, and p6* (data not shown). In contrast to the results obtained with the catalytically inactive precursor, efficient autoprocessing was detected in translation reactions directed by construct Gag-PR, which encodes wild-type PR (Fig. 2A, lane 3). The principal radiolabeled products were the MA-CA processing intermediate (p41), CA protein (p25/p24), and PR (11 kDa). They were identified by immunoprecipitation with antibodies against MA or CA (data not shown) and PR (lane 4). Although autoprocessing was efficient, the presence of residual precursor and processing intermediates indicated that it was incomplete.

Autoprocessing was very inefficient when PR was expressed as part of a precursor that lacked Gag sequences. Products generated from a construct that lacked most of the p6* domain but included the N-terminal F/P cleavage site of PR (Fig. 1, construct 1/4p6*PR, and Fig. 2B, lane 2) comigrated mainly with the sole translation product from the inactive control construct 1/4p6*PRA (Fig. 2B, lane 1). Only a small amount of processed 11-kDa PR was detected (Fig. 2B, lane 2 [arrowhead]). Precursors that contained the complete p6* domain (construct p6*PR) or, in addition, the distal Cys-His motif of NC (construct 1/2NC-PR) exhibited very little or no detectable autoprocessing activity in this assay (Fig. 2B, lanes 3 to 5).

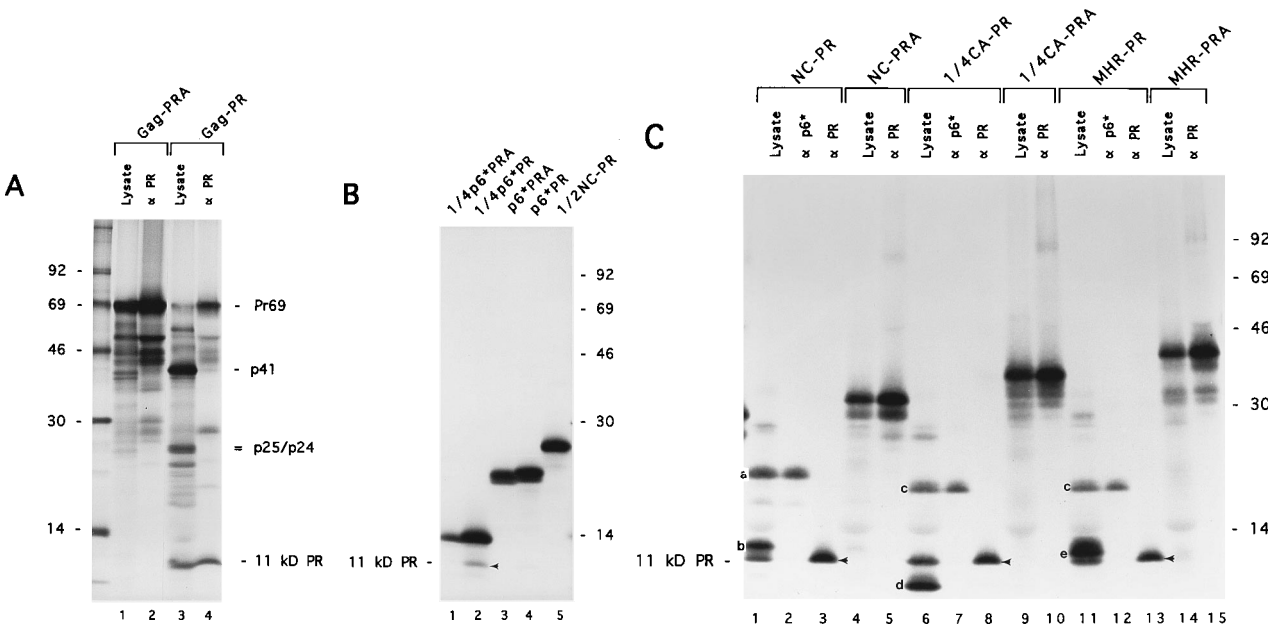

FIG. 2. SDS-PAGE analysis of autoprocessing of extended precursors. Total lysates were either analyzed directly (0.5 μl of lysate per lane) or after immunoprecipitation (4 μl of lysate per reaction) with antibody directed against PR, p6*, or CA. (A) Translation products of parental constructs Gag-PRA (lanes 1 and 2) and Gag-PR (lanes 2 and 3). Construct Gag-PRA contains an inactivating mutation of the active site residue (D-25 to A). Lanes: 1 and 3, total lysate; 2 and 4, lysate immunoprecipitated with anti-PR antibody. The positions of the full-length precursor, Pr69, and major processing products, p41 (MA-CA intermediate), p25 and p24 (CA proteins), and 11-kDa mature PR, are indicated on the right. (B) Translation of constructs exhibiting little or no autoprocessing activity. Since the globin protein present in RRL migrates with approximately the same mobility as some of the products, only products detected after immunoprecipitation with anti-PR antibody are shown. The position of the 11-kDa mature PR in the immunoprecipitated lysate is indicated. (C) Translation of constructs exhibiting efficient autoprocessing. Lanes: 1, 6, and 11, total lysate; 2, 7, and 12 and 3, 8, and 13, lysate immunoprecipitated with anti-p6* or anti-PR antibodies, respectively. The migration of mature 11-kDa PR is indicated by arrowheads. The migration of unprocessed precursors expressed from constructs encoding inactivated PRA, NC-PRA (lanes 4 and 5), 1/4CA-PR (lanes 9 and 10), and MHR-PRA (lanes 14 and 15), is shown. The molecular weights (in thousands) of marker proteins are indicated on the left (A) and right (B and C). The products generated by autoprocessing of cleavage sites in the precursors are indicated by letters a to e (for details, see the text).

Even after prolonged incubation at 30°C (up to 4 h), no autoproteolytic cleavage was detected at the N-terminal F/P site of PR, at the sites in p6* (39), or at the N/F site in the NC-p6* junction (37). The lack of proteolytic activity was not due to misfolding since these precursors were readily cleaved by exogeneously added purified HIV-1 PR (data not shown), indicating that the cleavage sites in the precursor were accessible. Moreover, p6*PR and 1/2NC-PR exhibited autoproteolytic activity upon overexpression in *E. coli* (data not shown), suggesting that they can function as enzymes when expressed at very high concentrations.

In contrast to these results, extremely efficient proteolytic activity with complete processing of PR-containing precursors was obtained with constructs that included the entire NC domain (construct NC-PR) or NC and additional upstream sequences (constructs 1/4CA-PR and MHR-PR) (Fig. 2C, lanes 1, 6, and 11). The efficiency was such that no residual PR-containing precursors were detected in the translation reaction mixture. The identity of the cleavage products was confirmed by immunoprecipitation with antibodies directed against PR (lanes 3, 8, and 13), p6* (lanes 2, 7, and 12), and the T7 tag (data not shown). In addition to the 11-kDa PR, autoprocessing of the cleavage sites present in precursor NC-PR generated products consisting of T7 tag–NC-p6* (product a, lanes 1 and 2) and T7 tag-NC (product b, lane 1). The p6* protein does not contain methionine residues and therefore could not be detected. Precursors 1/4CA-PR and MHR-PR produced NC-p6* (product c, lanes 6, 7, 11, and 12), NC (p7) (NC comigrated with the 11-kDa PR and could not be resolved in this gel system [data not shown]), T7 tag-1/4CA (product d, lane 6), and T7 tag-MHR (product e, lane 11). Only full-length precursors and precursors presumably initiated internally accumulated in lysates directed by the control constructs with inactivated PR (lanes 4 and 5, 9 and 10, 14 and 15).

Together these results demonstrate that autoprocessing of HIV-1 PR is influenced by regions located upstream of the PR domain. Whereas the presence of only the p6* domain appeared to be inhibitory, the addition of the NC (p7) domain resulted in a striking increase in PR autoprocessing. Thus, the p6* and NC domains had opposite effects on PR autoprocessing.

Dimerization activity of PR precursors. Since dimerization is necessary for PR activity, p6* and NC domains might influence the dimerization capability of PR-containing precursors. To test this possibility, we measured the protein-protein interactions of PR and the PR-containing precursors in the two-hybrid system (9). The two-hybrid system is based on the reconstitution of the activity of the yeast *Saccharomyces cerevisiae* GAL4 transcriptional activator. Protein-protein interaction is indicated by GAL4 promoter-dependent expression of the *lacZ* reporter gene. GAL4 hybrid proteins containing PR, p6*PR, and NC-PR polyproteins were constructed in the yeast vectors pMA424 (20) and pGAD (4), which contain the GAL4 DNA binding (residues 1 to 147) and activation (residues 768 to 881) domains, respectively. Since HIV-1 PR activity has been demonstrated previously in a similar system (23), we used the inactive version of PR (PRA) in all fusion constructs in this study to avoid PR autoprocessing from the GAL4 fusion domain. It has been reported that the mutated residue (Asp-25) does not affect PR dimerization (5). The fusion constructs were transformed into *S. cerevisiae* GGY1::171 (*MATα ura3-52 leu2-3, 112 his3-200 met*

TABLE 1. Reconstitution of GAL4 activity by GAL4 hybrid proteins[a]

Construct	β-Galactosidase activity (U)	No. of assays	σ
APR	≤4	5	<1
BPR	32.5	9	3.5
APR + BPR	71.1	17	5.5
APRΔ	≤4	5	<1
BPRΔ	≤4	5	<1
APRΔ + BPRΔ	≤4	5	<1
Ap6*PR	≤4	6	<1
Bp6*PR	98.2	7	5.6
Ap6*PR + Bp6*PR	124.3	5	12.9
ANC-PR	≤4	5	<1
BNC-PR	≤4	10	<1
ANC-PR + BNC-PR	228.0	5	71.6
SNF4-A + BSNF1	203.2	7	59.4

[a] Transformants grown in inducing medium (2% galactose, 2% ethanol, 2% glycerol) were disrupted by three cycles of freezing and thawing and resuspended in assay buffer (50 mM potassium phosphate [pH 7.8], 1 mM $MgCl_2$, 0.008% SDS) containing 8% (vol/vol) chloroform. Following the addition of the substrate, chlorophenol red–β-D-galactopyranoside (CPRG, 5 mM; Boehringer-Mannheim), and incubation at 30°C for 1 h, the absorption of the cleared supernatant was measured as the optical density at 574 nm. β-galactosidase activity was calculated according to method described by Miller (21) and represents the average activity determined from several different assays. The standard deviation of the mean (σ) is also shown. The inserts for all constructs were generated by PCR. The 3′ ends of all inserts except PRΔ were primed with oligonucleotide GAAGATCTATTAGAAGTTTAAAGTGC, which anneals at the end of the PR coding region. The 3′ end of the PRΔ insert was primed with oligonucleotide GAAGATCTCACTAACCAATCTGAGTCAAC, which anneals at positions 2082 to 2098 (HIV-1, strain BH10 [26]), resulting in a deletion of the last five residues of the PR coding region. The primers for the 5′ ends were oligonucleotides GGAAGATCTCCCCTCAGATCACTCTTTGGC (positions 1832 to 1850) for PR and PRΔ, GGGAAGATCTGGCCTTCC (positions 1636 to 1653) for p6*PR, and CGCGGATCCATGCAGAGAGGCAATTTTAGG (positions 1465 to 1485) for NC-PR.

mutant *tyr1 ade2 gal4D gal80D URA3*::*GAL1-lacZ*), which contains an integrated copy of the *GAL1-lacZ* reporter gene. Transformations were performed with the alkali-cation yeast transformation kit (Bio101, Inc., La Jolla, Calif.), and transformants were selected on minimal medium lacking histidine and leucine.

Initially, transformants were examined for β-galactosidase activity by filter assay. Yeast colonies were replica plated to filter paper, dipped in liquid nitrogen, and incubated in Z buffer containing 20 mM 5-bromo-4-chloro-3-indolyl-β-D-galactopyranoside (X-Gal) at 30°C. The activation of β-galactosidase expression results in cleavage of X-Gal and blue coloration of the yeast colonies. Cotransformation of the GAL4 activation domain hybrids (designated APR, Ap6*PR, and ANC-PR) and the GAL4 DNA binding domain hybrids (designated BPR, Bp6*PR, and BNC-PR) resulted in blue colonies when tested on filters. Since filter assays provide only qualitative information, we quantitated the β-galactosidase activity in single colonies grown in liquid culture. From each transformation a minimum of five different colonies was assayed (Table 1). Control experiments with the GAL4 hybrids of the yeast proteins SNF4 and SNF1, which are known to interact, resulted in an average of 203 U of β-galactosidase activity from cotransformants (Table 1), a value comparable to the previously reported activity of 180 U for these constructs (9). Control transformations with either one of the hybrid constructs alone or cotransformations of one hybrid together with vectors containing no insert did not result in any transcriptional activation.

Cotransformation of APR and BPR resulted in an average β-galactosidase activity of 71 U. However, transformation with BPR alone or with BPR and construct A without the insert also produced blue colonies in filter assays and 32.5 U of β-galactosidase activity in liquid culture (Table 1). The background activity of BPR was most likely due to nonspecific transcriptional activation mediated by the high beta sheet content of PR, since it has been reported that the transcriptional activation function of GAL4 is due to its β sheet conformation (31). This conclusion is supported by the fact that deletion of the five C-terminal residues of PR which contribute to formation of a 4-stranded antiparallel β sheet in the dimer (36) abolished the BPR background signal (Table 1, BPRΔ). This structure is critical for the stability of the PR dimer (32), and as expected, the deletion also obliterated PR-PR interaction (Table 1, APRΔ + BPRΔ).

Cotransformation of yeast cells with both GAL4-p6*PR hybrids induced levels of β-galactosidase that were increased in comparison to the levels induced by GAL4-PR hybrids (124 U) (Table 1). However, as in the latter case, transformation with the Bp6*PR hybrid alone or together with vector lacking the insert produced blue colonies in filter assays and significant levels of β-galactosidase activity (98 U).

Yeast cells coexpressing GAL4-NC-PR hybrids produced even higher levels of β-galactosidase activity than did PR and p6*PR hybrids (228 U) (Table 1). However, in contrast to the results obtained with BPR and Bp6*PR hybrids, BNC-PR exhibited negligible background activity (Table 1).

Yeast cells coexpressing GAL4-NC hybrids containing the NC (p7) domain alone showed no interaction (data not shown). While it is not clear why the hybrid NC construct did not interact, as the NC domain has been demonstrated previously to be important for Gag-Gag interaction (1, 10, 34), the results are consistent with the interpretation that the strong signal observed with the NC-PR hybrids was not due to interactions between the NC domains alone.

To examine protein-protein interactions in a more direct assay, tags consisting of six consecutive histidine residues were added to the amino terminus of precursors NC-PRA and p6*PRA. His-tagged and untagged precursors were translated in RRL in the presence of [^{35}S]methionine. Aliquots of control and cotranslation reaction mixtures were incubated with nickel-nitrilotriacetic acid (Ni-NTA)-affinity resin (Quiagen) in binding buffer at room temperature. Zinc chloride (1 mM) was included in the binding buffer to compete for nonspecific binding of the zinc fingers in NC to the nickel resin. Bound complexes were collected by centrifugation, washed, and eluted with a pH step gradient. Equal volumes of the eluants were analyzed by SDS-PAGE and fluorography. Protein-protein interactions were assayed by determining whether untagged precursors were retained on the resin by their interaction with tagged precursors.

The tagged 6xHisNC-PRA precursor was distinguished from the untagged NC-PRA precursor by its slightly slower migration during SDS–10% PAGE (Fig. 3). The 6xHisNC-PRA precursor bound efficiently to the resin and eluted at pH 5 to 4 (Fig. 3, lanes 1 to 7). Control experiments established that precursors did not elute at a pH above 5 and that no proteins remained bound after the last elution at pH 3.5 (data not shown). When cotranslation mixtures containing tagged and untagged precursors were incubated with the Ni-affinity resin (Fig. 3 lanes 8 to 14), a significant amount of untagged precursor was specifically retained on the resin and coeluted with the tagged precursor (lanes 11 to 13). Coelution peaked at pH 4, indicating strong and relatively acid-stable protein-protein interaction. The control experiment (lanes 15 to 21) demonstrated that this retention was dependent on the presence of

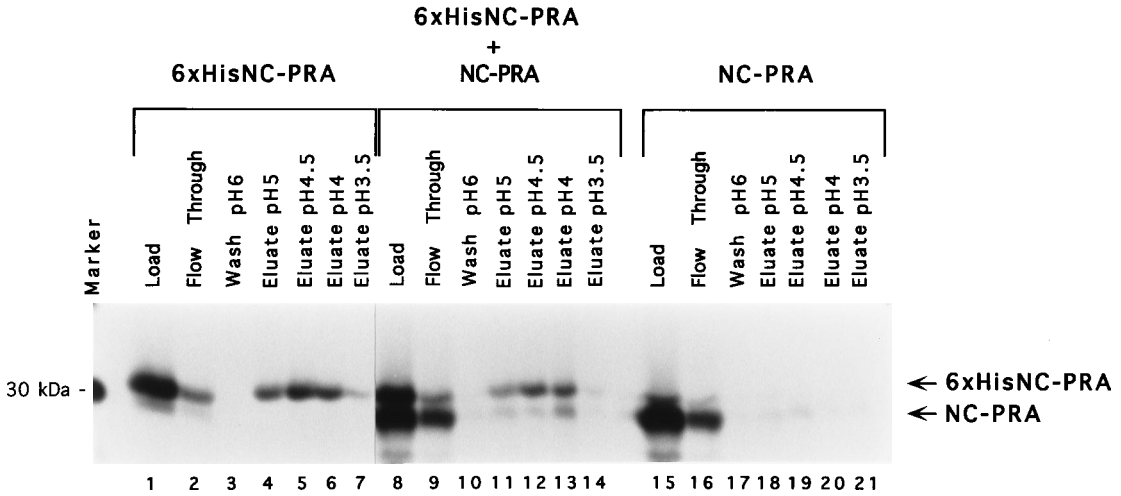

FIG. 3. Analysis of protein-protein interactions between 6xHis-tagged and untagged NC-PRA precursors by nickel-affinity binding and coelution. For construct 6xHisNC-PRA, the PCR fragment prepared for the construction of NC-PRA was ligated with plasmid pET-28a (Novagene) restricted with *Bam*HI and *Eco*RI. The insert was confirmed by sequencing. Insertion at *Bam*HI placed the coding sequence of NC-PRA behind a leader sequence coding for the 6xHis tag, a protease cleavage site for thrombin followed by the T7 tag (total length of leader, 33 amino acids). Purified DNA of constructs 6xHisNC-PRA or NC-PRA alone or of both constructs together was transcribed and translated in TNT T7 RRL (Promega) in the presence of [^{35}S]methionine. Each translation reaction mixture (6 μl) was incubated with Ni-NTA resin, washed, and eluted. Equal volumes of each fraction were mixed with SDS sample buffer, boiled, and analyzed by SDS–10% PAGE and fluorography. Lanes: 1, 8, and 15, aliquots of binding reaction mixtures removed for analysis prior to addition of Ni-NTA resin; 2, 9, and 16, flow-through fractions; 3, 10, and 17, wash fractions; 4 to 7, 11 to 14, and 18 to 21, eluted fractions. The positions of the 6xHisNC-PRA and NC-PRA precursors are indicated on the right.

the tagged precursor, since an amount of untagged precursor 1.5 times greater than the amount of the untagged precursor present in the cotranslation reaction resulted in only insignificant background binding. In addition, cotranslation experiments with decreasing amounts of tagged precursor led to a loss of detectable coelution (data not shown).

In contrast to the results obtained with NC-PRA, p6*PRA precursors failed to coelute with 6xHis-p6*PRA precursors when binding was examined by the same protocol (Fig. 4). Tagged 6xHis-p6*PRA precursors were readily distinguished from untagged p6*PRA by their slower migration during SDS–12.5% PAGE. Two additional bands migrating above and below 6xHis-p6*PRA were observed consistently (Fig. 4, lane 1). The more slowly migrating band was not related to the insert and appeared to be initiated elsewhere in the vector. The faster band was most likely the result of internal initiation in the T7 tag and did not contain the 6xHis tag. Precursor 6xHis-p6*PRA efficiently bound the resin and eluted with a peak at pH 4. No retention of the untagged precursor was observed when aliquots of cotranslation reaction mixtures were analyzed

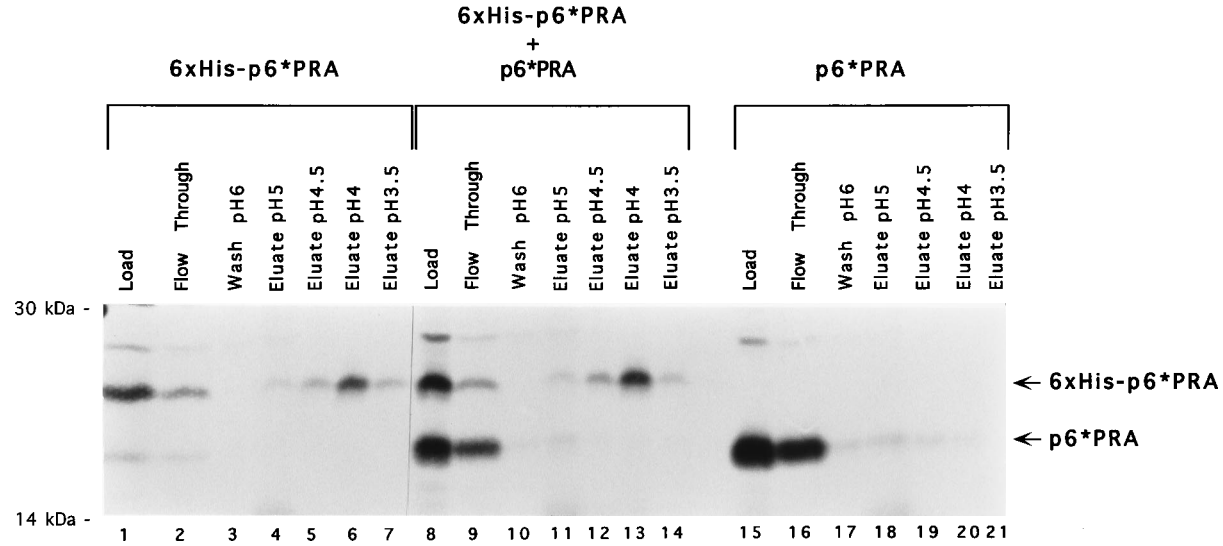

FIG. 4. Analysis of protein-protein interactions between 6xHis-tagged and untagged p6*PRA precursors by nickel-affinity binding and coelution. Construct 6xHis-p6*PRA was generated from construct p6*PRA by insertion of a linker coding for six histidines (CTAGTCATCACCATCACCATCACAGGC) at the unique *Nhe*I site of pET3 located at the 5′ end of the T7 tag-coding sequence. The correct orientation of the insert was confirmed by sequencing. Purified DNA of constructs 6xHis-p6*PRA or p6*PRA alone or of both constructs together was transcribed and translated in TNT T7 RRL (Promega) in the presence of [^{35}S]methionine. Binding and elution were as described in the legend to Fig. 3. Samples were analyzed by SDS–12.5% PAGE and fluorography. The positions of the 6xHis-p6*PRA and p6*PRA precursors are indicated on the right.

(Fig. 4, lanes 8 to 14). The control experiment (lanes 15 to 21) confirmed that the small amount of untagged p6*PRA precursor coeluting at pH 5 (lane 11) was due to background binding (lane 18). In additional cotranslation experiments, different ratios of tagged and untagged precursors did not improve the ability to bind untagged precursors (data not shown). Thus, the lack of detectable untagged precursor retained by the tagged precursor suggests that p6*PRA precursors did not interact efficiently.

These experiments confirm the results obtained with the GAL4 two-hybrid system, which indicated that the most efficient protein-protein interactions occur between NC-PRA precursors. Thus, the highly efficient autoprocessing activity of NC-PR correlated well with its strong protein-protein interaction.

These results demonstrate that regions upstream of the PR domain in a Gag-PR polyprotein of HIV-1 directly influence the autoprocessing activity of PR. It will be necessary to confirm the role of these regions in the context of full-length Gag-Pol; however, we concentrated our efforts on regions upstream of PR since regulatory domains would be expected to be translated before synthesis of the PR domain occurs. What is the mechanism by which NC facilitates PR autoprocessing? One possibility is that extension of p6*PR to the NC domain provided a critical length of N-terminal sequence required for accessibility or appropriate conformation of the cleavage site at the N terminus of PR. This possibility suggests that precursor length and not the NC sequence was important for efficient autoprocessing. However, we have observed that deletion of the NC domain in the context of Gag-PR prevents autoprocessing at the N-terminal F/P site of PR, indicating that NC sequences may play a more direct role (38). It is noteworthy that mutations in HIV-1 NC which affect PR activity or cleavage site accessibility have been reported previously (8, 19).

An alternative explanation, supported by our results with the GAL4 two-hybrid assay and nickel-affinity chromatography, is that the NC domain facilitates efficient dimerization of the PR domain. Such an effect could be mediated through stabilization of PR-PR interaction, since no signal for NC-NC interaction was detected in the GAL4 two-hybrid system. The fact that BNC-PR exhibited negligible β-galactosidase background activity, compared with that of BPR and Bp6*PR, suggests that changes in the conformation of the polyprotein upon addition of the NC domain masked the regions in PR responsible for nonspecific transcriptional activation. The NC protein complexes zinc and assumes a tightly structured conformation while the p6* domain appears to be unstructured (22, 29). Thus, the presence of a highly structured region juxtaposed with the p6* domain might stabilize PR dimerization. PR dimerization might also be facilitated by NC binding of RNA. Both specific and nonspecific RNA binding by NC has been reported previously (6, 7, 18) and could bring otherwise diffusible NC-PR precursors into close contact. Regions in NC have also been found to be important for protein-protein interactions of Gag precursors (10) and play a role in particle assembly of both HIV and Rous sarcoma virus (AD3) (1, 34). The effects on PR autoprocessing described here may be a reflection of this NC function. Thus, it appears that in addition to RNA packaging, the NC domain also functions during virus particle assembly and PR activation.

The presence of positive (i.e., NC) and negative (p6*) effector domains in Gag-Pol may provide a means of regulating autoprocessing to ensure spatial and temporal control of precursor cleavage. The Gag and Gag-Pol precursors of other retroviruses may include regions that play similar roles (2). In the case of HIV, we previously demonstrated that PR maturation from the precursor was required for efficient formation and release of mature particles (39). Thus, cleavage of Gag-Pol at sites that produce PR-containing intermediates with the NC domain may be an important determinant of PR maturation and thus formation of infectious viral particles.

We thank Stanley Fields and Paul Bartel for yeast strains and vectors, I. Jayatilaka for technical assistance, and C. Helmke for photography.

This work was supported by NIH grant GM 48294.

REFERENCES

1. **Bennett, R. P., T. D. Nelle, and J. W. Wills.** 1993. Functional chimeras of the Rous sarcoma virus and human immunodeficiency virus Gag proteins. J. Virol. **67:**6487–6498.
2. **Cameron, C. E., B. Grinde, J. Jentoft, J. Leis, I. T. Weber, T. D. Copeland, and A. Wlodawer.** 1992. Mechanism of inhibition of the retroviral protease by a Rous sarcoma virus peptide substrate representing the cleavage site between the *gag* p2 and p10 proteins. J. Biol. Chem. **267:** 23735–23741.
3. **Carter, C., and G. Zybarth.** 1994. Processing of retroviral Gag proteins: an *in vitro* approach. Methods Enzymol. **241:**227–253.
4. **Chien, C.-T., P. L. Bartel, R. Sternglanz, and S. Fields.** 1991. The two-hybrid system: a method to identify and clone genes for proteins that interact with a protein of interest. Proc. Natl. Acad. Sci. USA **88:**9578–9582.
5. **Darke, P. L., C. L. Dilanni, J. C. Heimbach, C.-T. Leu, V. M. Garsky, R. A. F. Dixon, and I. S. Sigal.** 1989. HIV-1 proteinase: substrates, inhibitors, and subunit interactions, p. 253–258. *In* H.-G. Kräusslich, S. Oroszlan, and E. Wimmer (ed.), Viral proteinases as targets for chemotherapy. Cold Spring Harbor Laboratory Press, Cold Spring Harbor, N.Y.
6. **Darlix, J.-L., C. Gabus, M.-T. Nugeyre, F. Clavel, and F. Barré-Sinoussi.** 1990. *cis* elements and *trans*-acting factors involved in the RNA dimerization of the human immunodeficiency virus HIV-1. J. Mol. Biol. **216:**689–699.
7. **deRocquigny, H., C. Gabus, A. Vincent, M.-C. Fournié-Zaluski, B. Roques, and J.-L. Darlix.** 1992. Viral RNA annealing activities of human immunodeficiency virus type 1 nucleocapsid protein require only peptide domains outside the zinc fingers. Proc. Natl. Acad. Sci. USA **89:**6472–6476.
8. **Dorfman, T., J. Luban, S. P. Goff, W. A. Haseltine, and H. G. Göttlinger.** 1993. Mapping of functionally important residues of a cysteine-histidine box in the human immunodeficiency virus type 1 nucleocapsid protein. J. Virol. **67:**6159–6169.
9. **Fields, S., and O. Song.** 1989. A novel genetic system to detect protein-protein interactions. Nature (London) **340:**245–246.
10. **Franke, E. K., H. E. H. Yuan, K. L. Bossolt, S. P. Goff, and J. Luban.** 1994. Specificity and sequence requirements for interactions between various retroviral Gag proteins. J. Virol. **68:**5300–5305.
11. **Jacks, T., M. D. Power, F. R. Masiarz, P. A. Luciw, P. J. Barr, and H. E. Varmus.** 1988. Characterization of ribosomal frameshifting in HIV-1 gag-pol expression. Nature (London) **331:**280–283.
12. **James, N. G., and A. R. Sielecki.** 1986. Molecular structure of an aspartic proteinase zymogen, porcine pepsinogen, at 1.8 Å resolution. Nature (London) **319:**33–38.
13. **Kaplan, A. H., M. Manchester, and R. Swanstrom.** 1994. The activity of the protease of human immunodeficiency virus type 1 is initiated at the membrane of infected cells before the release of viral proteins and is required for release to occur with maximum efficiency. J. Virol. **68:**6782–6786.
14. **Kaplan, A. H., and R. Swanstrom.** 1991. Human immunodeficiency virus type 1 Gag proteins are processed in two cellular compartments. Proc. Natl. Acad. Sci. USA **88:**4528–4532.
15. **Kohl, N. E., E. A. Emini, W. A. Schleif, L. J. Davis, J. C. H. A. F. Dixon, E. M. Scolnick, and I. S. Sigal.** 1988. Active human immunodeficiency virus protease is required for viral infectivity. Proc. Natl. Acad. Sci. USA **85:**4686–4690.
16. **Kräusslich, H.-G., H. Schneider, G. Zybarth, C. A. Carter, and E. Wimmer.** 1988. Processing of in vitro-synthesized *gag* precursor proteins of human immunodeficiency virus (HIV) type 1 by HIV proteinase generated in *Escherichia coli*. J. Virol. **62:**4393–4397.
17. **Laemmli, U. K.** 1970. Cleavage of structural proteins during the assembly of the head of bacteriophage T4. Nature (London) **227:**680–685.
18. **Luban, J., and S. P. Goff.** 1991. Binding of human immunodeficiency virus type 1 (HIV-1) RNA to recombinant HIV-1 *gag* polyprotein. J. Virol. **65:** 3203–3212.
19. **Luban, J., C. Lee, and S. P. Goff.** 1993. Effect of linker insertion mutations in the human immunodeficiency virus type 1 *gag* gene on activation of viral protease expressed in bacteria. J. Virol. **67:**3630–3634.
20. **Ma, J., and M. Ptashne.** 1987. A new class of yeast transcriptional activators. Cell **51:**113–119.

21. **Miller, J. H.** 1972. Experiments in molecular genetics. Cold Spring Harbor Laboratory Press, Cold Spring Harbor, N.Y.
22. **Morellet, N., N. Jullian, H. deRocquigny, B. Maigret, J.-L. Darlix, and B. P. Roques.** 1992. Determination of the structure of the nucleocapsid protein NCp7 from the human immunodeficiency virus type 1 by ^{1}H NMR. EMBO J. **11:**3059–3065.
23. **Murray, M. G., W. Hung, I. Sadowski, and B. DasMahapatra.** 1993. Inactivation of a yeast transactivator by the fused HIV-1 proteinase: a simple assay for inhibitors of the viral enzyme activity. Gene **134:**123–128.
24. **Partin, K., H.-G. Kräusslich, L. Ehrlich, E. Wimmer, and C. A. Carter.** 1990. Mutational analysis of a native substrate of the human immunodeficiency virus type 1 proteinase. J. Virol. **64:**3938–3947.
25. **Partin, K., G. Zybarth, L. Ehrlich, M. DeCrombrugghe, E. Wimmer, and C. Carter.** 1991. Deletion of sequences upstream of the proteinase improves the proteolytic processing of human immunodeficiency virus type 1. Proc. Natl. Acad. Sci. USA **88:**4776–4780.
26. **Ratner, L., W., Haseltine, R. Patarca, K. J. Livak, B. Starcich, S. F. Josephs, E. R. Doran, J. A. Rafalski, E. A. Whitehorn, K. Baumeister, L. Ivanoff, S. R. Petteway, M. L. Pearson, J. A. Lautenberger, T. S. Papas, J. Ghrayeb, N. T. Chang, R. C. Gallo, and F. Wong-Staal.** 1985. Complete nucleotide sequence of the AIDS virus HTLV-III Nature (London) **316:**277–284.
27. **Rhee, S. S., and E. Hunter.** 1987. Myristylation is required for intracellular transport but not for assembly of D-type retrovirus capsids. J. Virol. **61:**1045–1053.
28. **Smith, A. J., M.-I. Cho, M.-L. Hammarskjöld, and D. Rekosh.** 1990. Human immunodeficiency virus type 1 $Pr55^{gag}$ and $Pr160^{gag\text{-}pol}$ expressed from a simian virus 40 late replacement vector are efficiently processed and assembled into viruslike particles. J. Virol. **64:**2743–2750.
29. **South, T. L., P. R. Blake, R. C. Sowder III, L. O. Arthur, L. E. Henderson, and M. F. Summers.** 1990. The nucleocapsid protein isolated from HIV-1 particles binds zinc and forms retroviral-type zinc fingers. Biochemistry **29:**7786–7789.
30. **Studier, F. W., A. H. Rosenberg, and J. J. Dunn.** 1990. Use of T7 RNA polymerase to direct expression of cloned genes. Methods Enzymol. **185:**60–89.
31. **Van Hoy, M., K. K. Leuther, T. Kodadek, and S. A. Johnston.** 1993. The acidic activation domains of the GCN4 and GAL4 proteins are not α helical but form β sheets. Cell **72:**587–594.
32. **Weber, I. T.** 1990. Comparison of the crystal structures and intersubunit interactions of human immunodeficiency and Rous sarcoma virus proteases. J. Biol. Chem. **265:**10492–10496.
33. **Weiss, R., N. Teich, H. Varmus, and C. J.** 1982. RNA tumor viruses, vol. 1 and 2. Cold Spring Harbor Laboratory, Cold Spring Harbor, N.Y.
34. **Wills, J. W., C. E. Cameron, C. B. Wilson, Y. Xiang, R. P. Bennett, and J. Leis.** 1994. An assembly domain of the Rous sarcoma virus Gag protein required late in budding. J. Virol. **68:**6605–6618.
35. **Wills, J. W., and R. C. Craven.** 1991. Form, function, and use of retroviral Gag proteins. AIDS **5:**639–654.
36. **Wlodawer, A., M. Miller, M. Jaskolski, B. K. Sathyanarayana, E. Baldwin, I. T. Weber, L. M. Selk, L. Clawson, J. Schneider, and S. B. H. Kent.** 1989. Conserved folding in retroviral proteases: crystal structure of a synthetic HIV-1 PR. Science **245:**616–621.
37. **Wondrak, E. M., J. M. Louis, H. deRocquigny, J.-C. Chermann, and B. P. Roques.** 1993. The *gag* precursor contains a specific HIV-1 protease cleavage site between the NC (P7) and P1 proteins. FEBS Lett. **333:**21–24.
38. **Zybarth, G., and C. Carter.** Unpublished data.
39. **Zybarth, G., H.-G. Kräusslich, K. Partin, and C. Carter.** 1994. Proteolytic activity of novel human immunodeficiency virus type 1 proteinase proteins from a precursor with a blocking mutation at the N terminus of the PR domain. J. Virol. **68:**240–250.